Journal of Marine Science and Engineering

MDPI

Article

Effects of Phytoplankton Growth Phase on Settling Properties of Marine Aggregates

Jennifer C. Prairie *, Quinn W. Montgomery, Kyle W. Proctor and Kathryn S. Ghiorso

Department of Environmental and Ocean Sciences, University of San Diego, San Diego, 92110, CA, USA
* Correspondence: jcprairie@sandiego.edu

Received: 30 June 2019; Accepted: 7 August 2019; Published: 10 August 2019

Abstract: Marine snow aggregates often dominate carbon export from the surface layer to the deep ocean. Therefore, understanding the formation and properties of aggregates is essential to the study of the biological pump. Previous studies have observed a relationship between phytoplankton growth phase and the production of transparent exopolymer particles (TEP), the sticky particles secreted by phytoplankton that act as the glue during aggregate formation. In this experimental study, we aim to determine the effect of phytoplankton growth phase on properties related to aggregate settling. Cultures of the diatom *Thalassiosira weissflogii* were grown to four different growth phases and incubated in rotating cylindrical tanks to form aggregates. Aggregate excess density and delayed settling time through a sharp density gradient were quantified for the aggregates that were formed, and relative TEP concentration was measured for cultures before aggregate formation. Compared to the first growth phase, l ater phytoplankton growth phases were found to have higher relative TEP concentration and aggregates with lower excess densities and longer delayed settling times. These findings may suggest that, although particle concentrations are higher at later stages of phytoplankton blooms, aggregates may be less dense and sink slower, thus affecting carbon export.

Keywords: marine snow; biological pump; TEP; carbon export; biogeochemical cycling

1. Introduction

Vertical carbon flux via the biological carbon pump removes more than 10 billion tons of carbon from the surface ocean every year, playing a major role in biogeochemical cycling and regulating global climate [1]. The primary mechanism driving the export of this particulate organic carbon (POC) is the coagulation of organic matter into aggregates, or marine snow, which can sink at rates one hundred times faster than individual phytoplankton cells [2]. However, differences in the concentration, composition, and other properties of marine snow cause large variations in the efficiency of the biological pump both temporally and spatially [3].

Previous studies have observed that many biological and physical factors affect aggregate formation [4], including phytoplankton and bacteria community composition [5,6], temperature [7], turbulence [8,9], and phytoplankton physiology [10]. In addition to affecting aggregation directly, these factors can affect the production and accumulation of transparent exopolymer particles (TEP), sticky gel-like particles that are secreted by phytoplankton and bacterial cells and allow phytoplankton and other particulate matter to stick together when they collide, thus playing an essential role in aggregate formation [11,12].

The effect of phytoplankton growth phase on aggregation and carbon export is of particular interest because of its relation to phytoplankton blooms, which can often drive large pulses of exported POC [13–15]. Previous studies have found that phytoplankton growth phase, in addition

to phytoplankton species, affects TEP production and subsequently aggregate formation [16]. Cultures of the diatom *Thalasiosira weissflogii* (along with other species) were found to have much higher TEP concentrations during the later growth phases, although the increase in TEP was much more moderate when it was normalized by cell concentration [16]. Similarly, higher TEP production per cell has been observed for *Synechococcus* under nutrient limitation [17]. Other experiments with *Thalasiosira weissflogii* found that TEP production may also depend on growth rate [18]. These studies, in conjunction with others that have found higher sticking efficiency during aggregation in later growth phases [10,19], have demonstrated a clear link between phytoplankton growth phase and aggregate formation. However, it is still not understood how phytoplankton growth phase affects the properties of the aggregates that are formed. Given that TEP can impact aggregate density, with higher TEP concentrations resulting in lower sinking velocities [12,20], carbon export through aggregate settling may vary significantly for different growth phases, and thus at different stages of phytoplankton blooms. In addition, less dense aggregates are more likely to have reduced sinking velocities as they pass through sharp density gradients, a phenomenon referred to as delayed settling [21,22], allowing thin layers of aggregates to form [23,24], which will further affect carbon remineralization and export.

In this study, we examine the effect of growth phase of the diatom *Thalasiosira weissflogii* on aggregate excess density (that is closely related to settling velocity), relative TEP concentration, and delayed settling time of aggregates through a sharp density gradient. We then investigate the relationships between these properties to gain insight into the connection between phytoplankton bloom dynamics and carbon export through aggregate settling.

2. Materials and Methods

In the summers of 2015 and 2017, four experiments were conducted to investigate the properties of aggregates formed from phytoplankton at different growth phases (Table 1). Three different aggregate properties were measured: (1) aggregate excess density, , defined as the difference between the density of the aggregate, , and the density of the fluid it is settling in, in all four experiments, (2) relative TEP concentration in Experiments 3 and 4, and (3) the delayed settling time of aggregates through a sharp density gradient in Experiment 2.

Table 1. Description of the four experiments conducted with the experiment start date, the number of days each culture was grown before stopped for each growth phase (GP1-early exponential, GP2-late exponential, GP3-early stationary, and GP4-late stationary), the aggregate properties that were measured, and the number of aggregates measured for excess density for each growth phase.

Experiment Number	Experiment Start Date	Days Each Culture was Grown Before Stopped	Aggregate Properties Measured	Number of Aggregates for Excess Density Measurements
1	16 June 2015	GP1: 6 GP2: 10 GP3: 13 GP4: 16	excess density	GP1: 15 GP2: 22 GP3: 16 GP4: 17
2	28 July 2015	GP1: 6 GP2: 10 GP3: 13 GP4: 16	excess density, delayed settling time	GP1: 17 GP2: 19 GP3: 13 GP4: 15
3	1 August 2017	GP1: 5 GP2: 9 GP3: 12 GP4: 15	excess density, TEP concentration	GP1: 6 GP2: 6 GP3: 5 GP4: 2

4	12 August 2017	GP1: 5 GP2: 9 GP3: 12 GP4: 15	excess density, TEP concentration	GP1: 17 GP2: 5 GP3: 9 GP4: 6

2.1. Growth of Phytoplankton Cultures and Formation of Aggregates

In all experiments, xenic cultures of the diatom species *Thalasiosira weissflogii* (CCMP1050, obtained from the National Center for Marine Algae and Microbiota) were used; this species was chosen since it is a common bloom-forming diatom that has been shown to have variations in TEP production for different growth phases [16]. Cultures were grown in f/2 media at room temperature on a 12:12 h light:dark cycle. Four cultures were started at the same time (each in a separate 2 L flask) and were stopped on different days representing four different growth phases (Table 1). The growth of the cultures was monitored by measuring in vivo fluorescence (Trilogy Laboratory Fluorometer, Turner Designs, San Jose, CA, USA) daily, (although in a few cases in Experiment 3 the measurements were taken every other day). In Experiment 4, cell concentration was also measured daily with a particle counter (Multisizer 3 Coulter Counter, Beckman Coulter, Indianapolis, IN, USA). Based on fluorescence and cell concentration measurements, the four growth phases represent distinct stages of the phytoplankton growth curve, and hereafter the four growth phases are referred to as GP1-early exponential, GP2-late exponential, GP3-early stationary, and GP4-late stationary, respectively (Figure 1).

When each culture was stopped, a cell count was conducted with the Coulter Counter and the culture was diluted with filtered seawater (to a concentration of 25,000 cell/mL for Experiments 1 and 2, 35,000 cells/mL for Experiment 3, and 20,000 cells/mL for Experiment 4). The diluted culture was transferred into a cylindrical acrylic tank with a volume of 2.2 L and circumference of 51 cm. The cylindrical tank was then incubated on a roller table (Wheaton) where it rotated at a speed of 3.3 RPM to induce aggregate formation, a method which has been widely used in previous studies [21,25]. The tanks were incubated in complete darkness to prevent further growth of the phytoplankton cultures during aggregate formation, and the total time of incubation was 3 days in Experiments 1 and 2 and 2 days in Experiments 3 and 4.

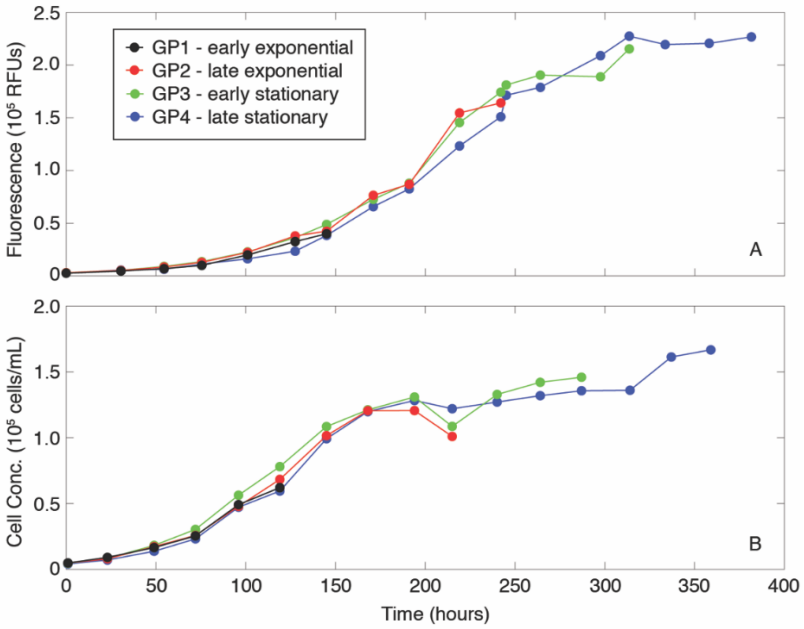

Figure 1. Example growth curves of *T. weissflogii* for (**A**) Experiment 1, showing measurements of fluorescence (in raw fluorescence units) vs time, and (**B**) Experiment 4, showing measurements of cell concentration vs time. Colors represent the four different growth phases (GP1-early

exponential, GP2-late exponential, GP3-early stationary, and GP4-late stationary) as indicated in the legend.

2.2. Measuring Aggregate Excess Density

In all experiments, aggregate excess density was measured for aggregates in each growth phase by quantifying the size and settling velocity of individual aggregates following the method described in References [21,22]. In Experiments 3 and 4, the aggregates were very fragile for some of the growth phases resulting in lower sample sizes (Table 1); it is possible that in these experiments, aggregate density measurements may have been biased because aggregate density could not be quantified for the more fragile aggregates which may have been less dense on average. In particular, for GP4-late stationary of Experiment 3 the excess densities of only two aggregates were successfully measured and so this growth phase was not included in statistical analyses. After the aggregates were incubated on the roller table, the cylindrical tank was placed upright and aggregates were allowed to slowly settle to the bottom of the tank. Individual aggregates were removed with a volumetric pipette with the tip partially cut off so the opening was a few mm in diameter. Aggregates were placed on a Sedgwick rafter slide with a millimeter square grid and photographed with a digital microscope (Model 26700-300) (Aven, Ann Arbor, MI, USA). From the images taken with the digital microscope, the equivalent spherical diameter (ESD) of each aggregate was found by quantifying the cross-sectional area of the aggregate in MATLAB (Version 2015, MathWorks, Natick, MA, USA) and assuming that it represented that of an equivalently sized sphere. Since the aggregates are irregularly shaped and the images provide just a 2-dimensional projection of each aggregate, the ESD of each aggregate measured with this method is likely an overestimate [21]. Figure 2 provides example images of aggregates from each growth phase, although shape and size can vary between aggregates, so the images are not necessarily representative of aggregates from that growth phase. Aggregates sizes are not presented as part of the results but were used to calculate aggregate excess density as described below, and ESD of each aggregate used for aggregate density measurements are reported in the full data available as part of the Supplementary Material.

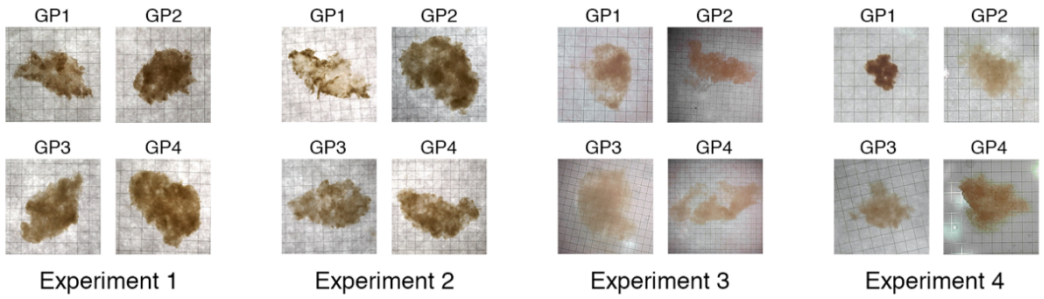

Figure 2. Images of example aggregates from each growth phase in each experiment. Aggregates are shown on a millimeter square grid.

After each aggregate was imaged for measuring its size, sinking velocity of the aggregate was determined by carefully dropping the aggregate into a rectangular acrylic tank with a 15 cm × 15 cm base and a 60 cm height filled with filtered seawater of a similar density to the water in which the aggregates were formed. All water densities were measured using a DMA 35 Portable Density Meter (Anton Paar, Graz, Austria). The trajectory of the aggregate as it settled through the tank was recorded by video (in Experiments 1 and 2 using a Sony Alpha 7 camera and in Experiments 3 and 4 using a Point Grey Grasshopper camera Model GS3-U3-41C6NIR-C), with a recording rate of 29 frames/s (Experiments 1 and 2) or 20 frames/s (Experiments 3 and 4). Images were analyzed with MATLAB and sinking velocity () was calculated from the vertical displacement of the aggregate over at least 6 continuous seconds, using an image of a ruler to linearly correct

pixels to cm. Then aggregate excess density, , was calculated according to the equation from Reference [26]:

, (1)

where is the acceleration due to gravity, *d* is the ESD of the aggregate, is the density of the fluid, and is the drag coefficient calculated using the empirical drag law:

, (2)

where Re is the Reynolds number calculated as:

, (3)

where is the kinematic viscosity of seawater (using the value cm^2/s at 20 °C). It is important to note that aggregates are very porous (usually over 99% water by volume), and so the excess density of aggregates as quantified here is a function of both the density of the solid matter within the aggregate and its porosity [27].

2.3. Measuring Relative TEP Concentration

In Experiments 3 and 4, relative TEP concentration was measured for each growth phase using the colorimetric method described in References [28,29]. After each culture was stopped (but before it was diluted and added to the cylindrical tank for aggregate formation), four 10 mL samples of the culture were each filtered onto a 0.4 µm polycarbonate filter, stained with a dye solution (aqueous solution of 0.02% alcian blue, 8 GX, and 0.06% acetic acid), and rinsed with deionized water. Additionally, four empty filters for each growth phase were also stained with the same dye and rinsed with deionized water in order to act as blanks. Filters were stored in centrifuge tubes in the freezer until the end of the experiments (about one month). Filters were then individually immersed in 80% sulfuric acid for two hours and absorbance was read in a spectrophotometer at 787 nm. The average absorbance of the blanks for each growth phase was subtracted from each sample absorbance value. The absorbance values in this study were not calibrated (which is typically done with a standard of gum xanthan [28]); however, absorbance has been shown to be linearly related to mass of gum xanthan [28], and so these absorbance values represent relative TEP concentration, which can be compared to the other growth phases in the same experiment (since the same batch of dye was used throughout an experiment). To better compare TEP concentration to aggregate properties, relative TEP concentration was also normalized by the cell concentration of the culture at the time the samples were taken, since during aggregate formation all cultures in each experiment were diluted to the same concentration before incubating on the roller table.

2.4. Measuring Delayed Settling Time of Aggregates at Sharp Density Gradients

In Experiment 2, delayed settling time through a sharp density gradient was measured for 5–7 aggregates per growth phase using the method described in References [21,22]. Briefly, a two-layer water column was set up with a sharp density transition in the middle of a tank of the same size as used for the aggregate excess density measurements. To create the density gradient, top layer fluid (of approximately the same density as the fluid in which the aggregates were formed) was carefully poured through a diffuser on top of denser bottom layer fluid (that was created by adding Instant Ocean sea salt to filtered seawater). In GP1-early exponential and GP2-late exponential the bottom layer fluid had a density 0.0046 g/cm^3 greater than that of the top layer fluid, and in GP3-early stationary and GP4-late stationary the bottom layer fluid had a density 0.0035 g/cm^3 greater than that of the top layer fluid. The trajectory of each aggregate was recorded in the same way as for the excess density measurements (using a Sony Alpha 7 camera recording at 29 frames/s). Using MATLAB, and again correcting pixels to cm from the measured field of view of the camera, the settling velocity of the aggregate over time was calculated from its

vertical displacement and was then smoothed over a 1 s span. All aggregates in this experiment came to a complete stop (settling velocity of 0 cm/s) at or near the density gradient. The delayed settling time (DST) in seconds was calculated as in Reference [21], defined as the length of time that the aggregate's smoothed settling velocity was less than 90% of the settling velocity in the bottom layer (calculated as the average settling velocity over at least 3 s when the aggregate was near the bottom of the field of view).

3. Results

Mean excess density of aggregates was found to significantly differ between growth phases for all four experiments (ANOVA, Experiment 1 $p < 0.0001$, Experiment 2 $p < 0.0001$, Experiment 3 $p = 0.0002$, Experiment 4 $p < 0.0001$) (Figure 3). In every experiment, the excess density of aggregates was significantly higher in GP1-early exponential than all other growth phases according to a Tukey's post-hoc test. In Experiment 4, the mean excess density of aggregates in GP1-early exponential was more than ten times larger than those of the other growth phases, and there was a noticeable difference in the appearance of aggregates from that growth phase (Figure 2); however, the differences in mean excess density for the other experiments were more moderate.

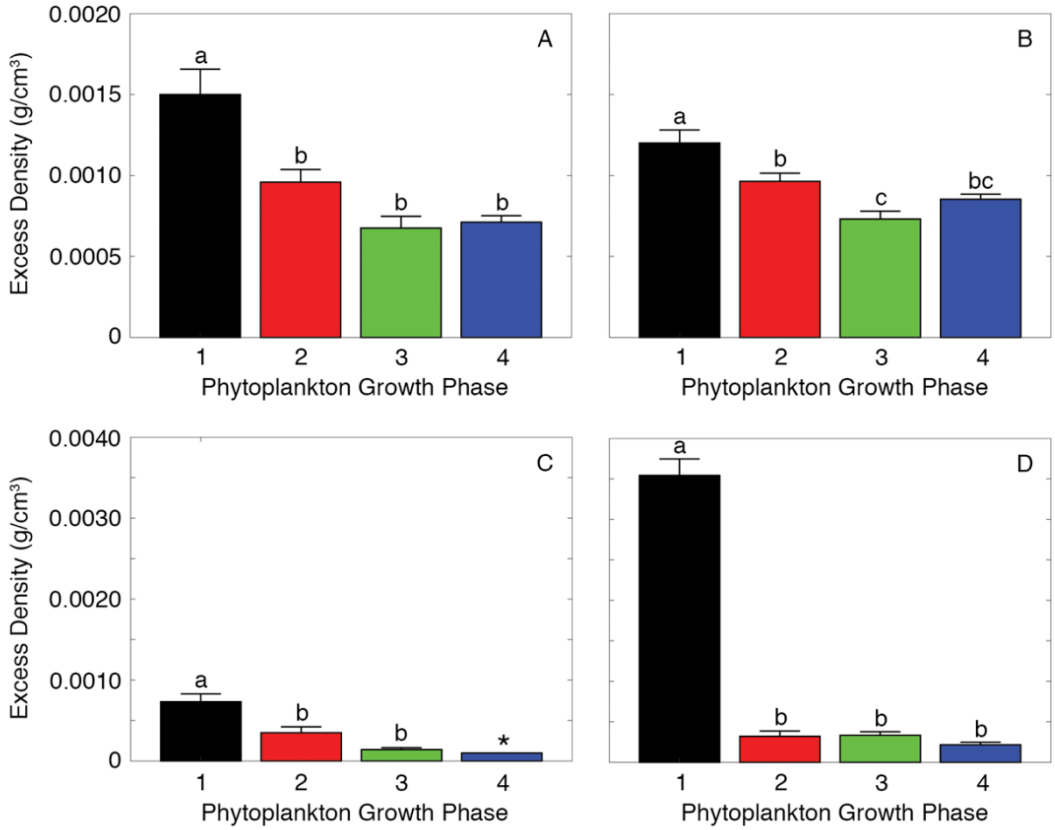

Figure 3. Excess aggregate density for each of the four growth phases in each of the four experiments: (**A**) Experiment 1 (**B**) Experiment 2 (**C**) Experiment 3 (**D**) Experiment 4. In each panel, the height of the bar gives the mean excess density for that growth phase and the error bars represent one standard error. The lowercase letters above the bars indicate the results of a Tukey's post-hoc test with a significance level of 0.05: growth phases that share a letter do not have significantly different means and growth phases that do not share a letter do have significantly different means. The asterisk above GP4 in Experiment 3 indicates that this data was not included in the ANOVA analysis because of low sample size.

Relative TEP concentration for the phytoplankton cultures significantly differed between growth phases for both Experiments 3 and 4 (ANOVA, Experiment 3 $p < 0.0001$, Experiment 4 $p < 0.0001$) (Figure 4A,B). In both experiments, relative TEP concentration was significantly lower in GP1-early exponential than all other growth phases according to a Tukey's post-hoc test. A significant difference between growth phases was also found for relative TEP concentration when normalized by cell concentration (ANOVA, Experiment 3 $p = 0.0009$, Experiment 4 $p = 0.036$) (Figure 4C,D). Normalized relative TEP was lower in GP1-early exponential than GP2-late exponential, but the differences were more moderate and no difference was observed between GP1-early exponential and GP3-early stationary or GP4-late stationary.

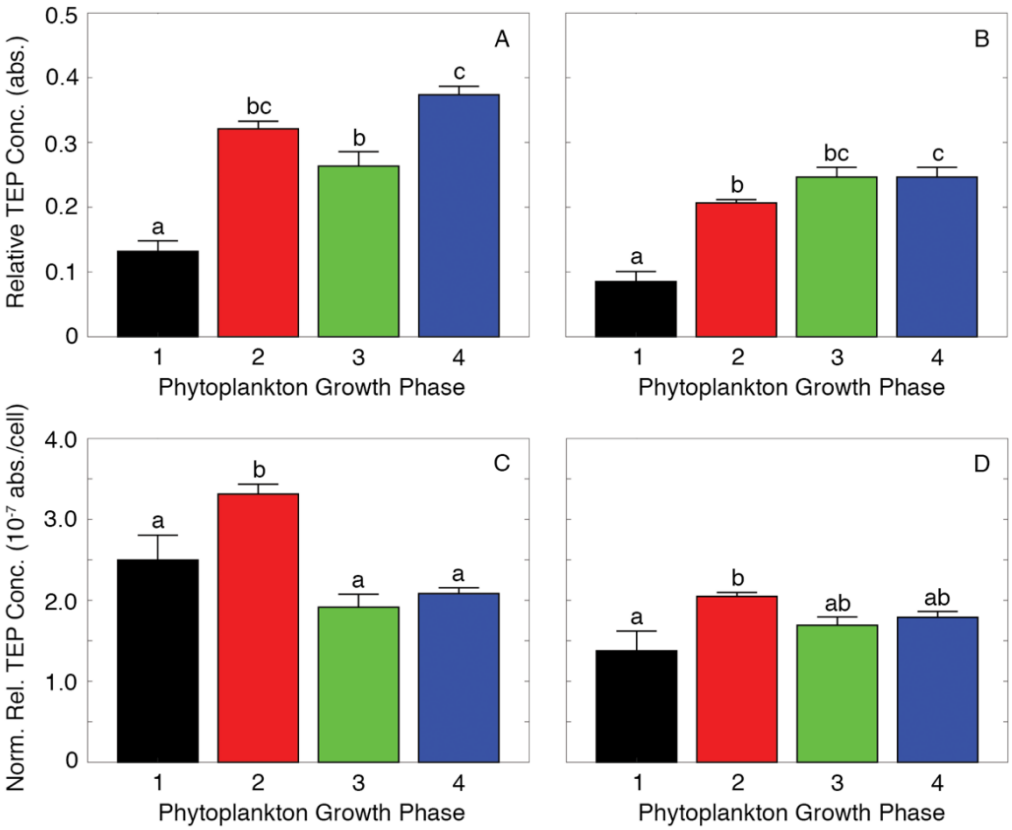

Figure 4. (**A**) Relative TEP concentration for each growth phase in Experiment 3. (**B**) Relative TEP concentration for each growth phase in Experiment 4. (**C**) Normalized relative TEP concentration for each growth phase in Experiment 3. (**D**) Normalized relative TEP concentration for each growth phase in Experiment 4. In each panel, the height of the bar gives the mean TEP concentration for that growth phase and the error bars represent one standard error. The lowercase letters above the bars indicate the results of a Tukey's post-hoc test with a significance level of 0.05: growth phases that share a letter do not have significantly different means and growth phases that do not share a letter do have significantly different means.

When mean excess density was plotted against mean relative TEP concentration for all growth phases in Experiments 3 and 4, a negative correlation was found ($p = 0.038$), even when the outlier data point from Experiment 4 GP1-early exponential was excluded ($p = 0.040$) (Figure 5A). No correlation was found between mean excess density and mean normalized relative TEP concentration ($p = 0.29$) (Figure 5B).

There was a significant difference in the delayed settling time of aggregates through a sharp density gradient between growth phases in Experiment 2 (ANOVA, $p < 0.0001$), and the mean of each growth phase significantly differed from every other growth phase according to a Tukey's post-hoc test, with the lowest delayed settling time observed for GP1-early exponential (Figure

6A). When delayed settling time was plotted against mean excess density for each growth phase, no clear relationship was found (Figure 6B), although only four data points were included since delayed settling time was measured in Experiment 2 only.

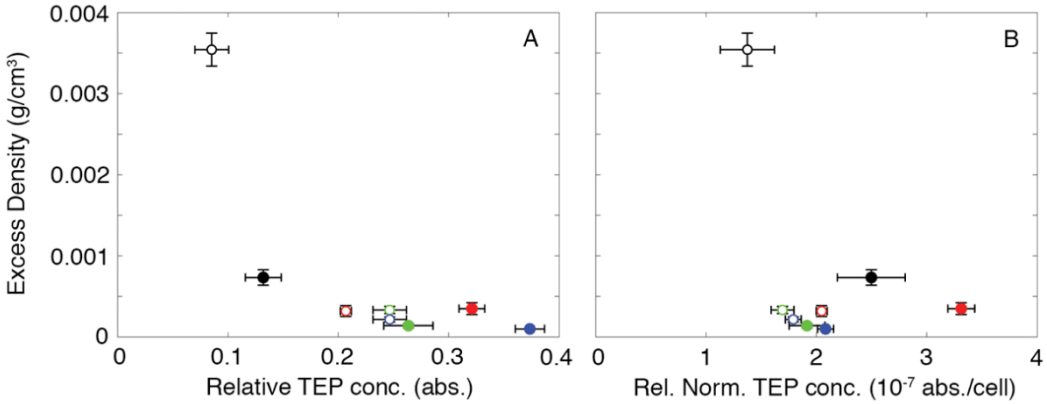

Figure 5. (**A**) Mean aggregate excess density vs mean relative TEP concentration. (**B**) Mean aggregate excess density vs mean normalized relative TEP concentration. In both panels, closed circles represent data from Experiment 3 and open circles represent data from Experiment 4, with colors indicating growth phase (see legend in Figure 1). Vertical and horizontal error bars represent plus or minus one standard error in the respective variables.

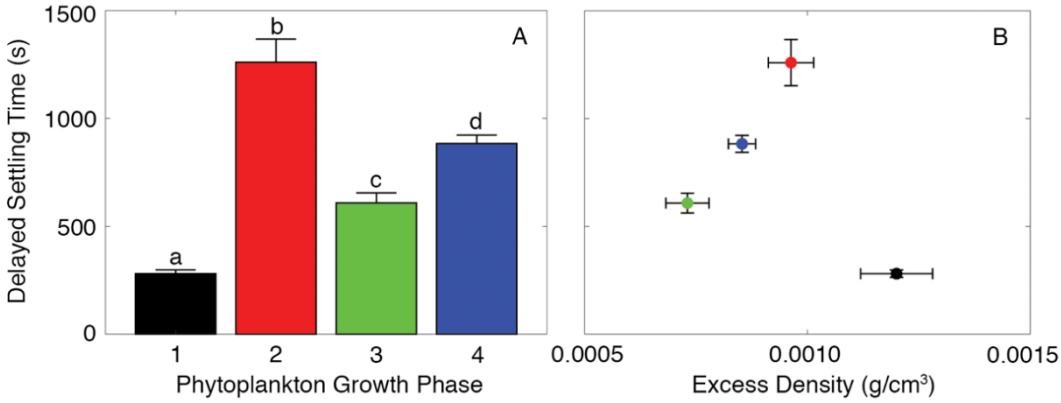

Figure 6. (**A**) Mean delayed settling time for each of the four growth phases in Experiment 2. Error bars represent one standard error. Number of aggregates measured in each growth phase was 7 for GP1, 5 for GP2, 7 for GP3, and 5 for GP4. Note that the density gradient in settling experiments for GP1 and GP2 was sharper than that of settling experiments for GP3 and GP4. The lowercase letters above the bars indicate the results of a Tukey's post-hoc test with a significance level of 0.05: growth phases that share a letter do not have significantly different means and growth phases that do not share a letter do have significantly different means. (**B**) Mean delayed settling time vs mean aggregate excess density for experiment 2. Colors indicate growth phase (see legend in Figure 1). Vertical and horizontal error bars represent plus or minus one standard error in the respective variables.

4. Discussion

The results of this study indicate that phytoplankton growth phase can significantly impact properties related to aggregate settling. In each of the four experiments, higher aggregate excess density was observed in GP1-early exponential compared to all other growth phases. These patterns may be explained by relative TEP concentration, which was found to be higher in the later growth phases, consistent with findings from previous studies [10,16]. The density of TEP is lower than that of seawater [12,30], and so it is logical that the formation of aggregates in

later growth phases with higher concentrations of TEP present would lead to reduced aggregate densities and consequently lower settling velocities [20,31]. However, since aggregate formation in our experiments was conducted with phytoplankton concentration held constant, relative TEP concentration normalized per cell is likely the more relevant measure, and the relationship between normalized relative TEP concentration and growth phase was less clear. The potential connection between higher TEP concentration within the phytoplankton cultures and lower aggregate density suggests an increased presence of TEP within the aggregates; however, the content of TEP in individual aggregates was not quantified in this study. Previous studies have used microscopy to determine the number and sizes of TEP within aggregates [29], and future research applying these methods would be valuable to confirming whether growth phase impacts the presence of TEP within aggregates specifically. It is also important to note that TEP production has been linked not only to phytoplankton physiology, but also to the composition of the associated bacterial community [32], and in some cases, including for the diatom used in this study, the presence of bacteria is required for aggregation to occur [33]. Moreover, other forms of extracellular polymeric substances (EPS) that affect aggregation and likely aggregate settling may also be affected by phytoplankton physiology and other factors [34]. Therefore, further work will be needed to untangle the relationship between phytoplankton growth phase, bacterial assemblage, TEP and other EPS both within the water column and within aggregates, and aggregate density.

The link between phytoplankton growth phase, TEP concentration, and aggregate excess density may help explain some of the large variability in aggregate settling velocity in natural environments [35,36], since excess density, along with particle size and shape, is one of the main factors that determines an aggregate's settling velocity in the ocean. In addition to TEP, aggregate composition more generally will affect aggregate density and should be investigated in relation to other factors. In particular, recent research has shown that marine snow can be a transport vehicle for oil [37] and plastics [38,39], and these low density substances can further affect the sinking velocity of aggregates.

In addition to excess density and TEP concentration, phytoplankton growth phase also impacted the delayed settling time of aggregates as they passed through a sharp density gradient, with aggregates formed from phytoplankton at the later growth stages exhibiting a longer period of decreased sinking velocity. An important consideration is that the density gradient used in delayed settling measurements for GP1-early exponential and GP2-late exponential was sharper than that used in delayed settling measurements for GP3-early stationary and GP4-late stationary, so the delayed settling time for aggregates between these pairs of growth phases may not be comparable. However, delayed settling time for aggregates is typically longer when passing through sharper density gradients [22], and so if the delayed settling measurements in GP3-early stationary and GP4-late stationary were conducted with an equally strong density gradient as the earlier growth phases, the delayed settling times would likely be even greater. The increased delayed settling time at later growth phases is expected given a previous experimental study that found longer periods of decreased velocities through sharp density gradients for aggregates of lower densities [22]. Although the density gradients used in these experiments are unrealistically sharp compared to natural environments, this pattern in delayed settling behavior suggests that aggregates formed from phytoplankton in later growth phases may be more likely to form layers [23], which have been shown to serve as hotspots for bacterial activity and carbon remineralization [40] and potentially for zooplankton grazing [41].

The findings of this study demonstrate that multiple properties of aggregates related to their settling and ultimately carbon export are affected by phytoplankton growth phase. Although our results are based on laboratory experiments, there are important potential implications for the transport of POC from the surface ocean during phytoplankton blooms. Aggregation and carbon export is typically associated with the termination of phytoplankton blooms, since at this stage

high particle concentrations and large quantities of TEP will induce aggregate formation [42]. However, although aggregates may be more abundant in the later stages of the bloom, the results of this study suggest that these aggregates may contain more TEP and have lower excess densities, thus sinking slower (Figure 7). Moreover, less dense aggregates at the end of a phytoplankton bloom may more commonly form thin layers, potentially allowing for higher rates of remineralization. Lastly, changes in aggregate settling properties due to phytoplankton growth phase could be further impacted by temperature and pH [43–45], which will play a key role in the context of a changing climate. The relationships observed in this study provide important insight into the mechanistic link between growth phase and local carbon export for a common bloom-forming diatom by investigating aggregate properties related to settling, and future field and modeling studies will be valuable in further determining the impacts to biogeochemical cycling on larger scales.

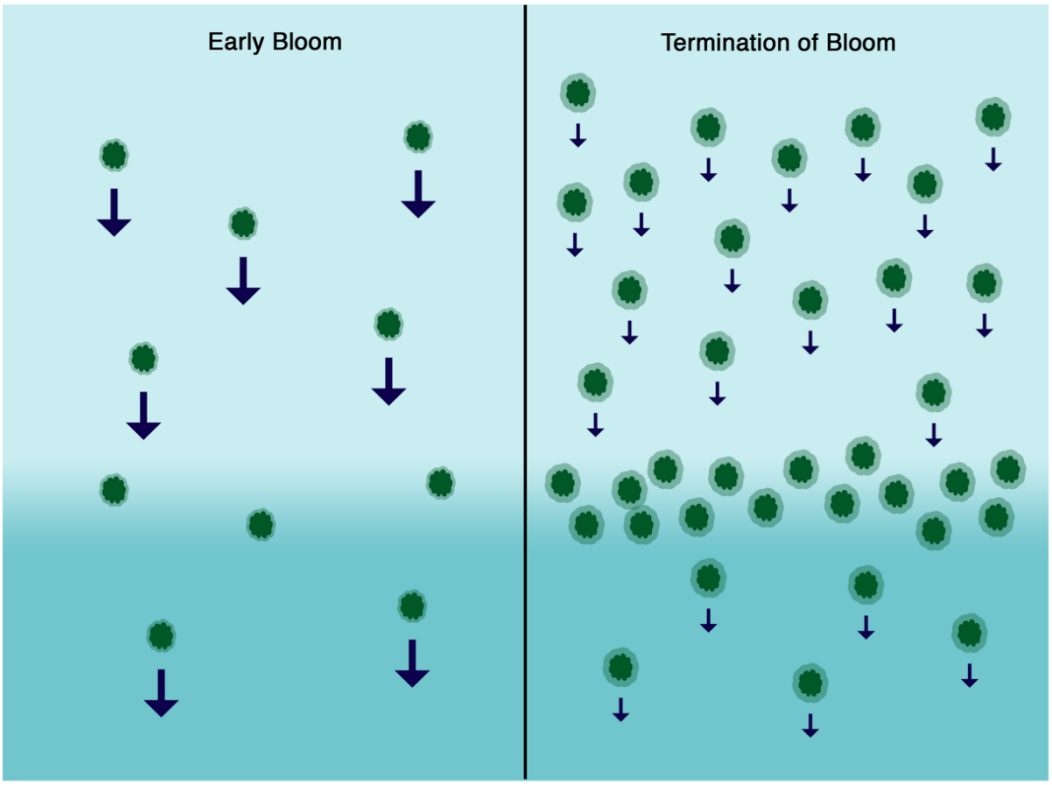

Figure 7. A schematic showing the potential implications of changes in aggregate settling properties for different phytoplankton growth phases. In the early stages of a phytoplankton bloom, aggregates contain less transparent exopolymer particles (TEP, indicated by light green border around dark green aggregates), sink faster (velocity indicated by size of downward arrows), and do not slow down as long at density gradients (density of water indicated by blue shading). At the end of a bloom, aggregates have higher concentrations of TEP, are less dense and thus sink slower, and can slow down for longer periods of time at sharp density gradients creating layers.

Supplementary Materials: All data presented in this manuscript are available online at www.mdpi.com/xxx/s1, in Excel file format, including: Aggregate_Density_Data, TEP_Data, and Aggregate_DelayedSettling_Data.

Author Contributions: Conceptualization, J.P.; methodology, J.P., Q.M., K.P. and K.G.; formal analysis, J.P., Q.M., K.P. and K.G.; writing—original draft preparation, J.P.; writing—review and editing, J.P., Q.M., K.P. and K.G.; supervision, J.P.; project administration, J.P..; funding acquisition, J.P.

Funding: This research was funded by National Science Foundation (NSF), grant number OCE-1335088, and additionally by NSF-CAREER, grant number OCE-1654276.

Acknowledgments: We would like to thank Ciera Villegas, Andrea Mast, Riley Henning, and Grace Cawley for help with experimental work, and Kai Ziervogel, Wilton Burns, Adrian Marchetti, and Brian White for their valuable feedback. Thanks to Uta Passow and Julia Sweet for their help with TEP quantification methodology. In addition, we would like to thank two anonymous reviewers, whose comments greatly improved this manuscript.

Conflicts of Interest: The authors declare no conflict of interest.

References

1. Turner, J.T. Zooplankton fecal pellets, marine snow, phytodetritus and the ocean's biological pump. *Prog. Oceanogr.* **2015**, *130*, 205–247.
2. Alldredge, A.L.; Silver, M.M. Characteristics, Dynamics and Significance of Marine Snow. *Prog. Oceonogr.* **1988**, *20*, 41–82.
3. De La Rocha, C.L.; Passow, U. Factors influencing the sinking of POC and the efficiency of the biological carbon pump. *Deep Sea Res. Part II Top. Stud. Oceanogr.* **2007**, *54*, 639–658.
4. Burd, A.B.; Jackson, G.A. Particle Aggregation. *Annu. Rev. Mar. Sci.* **2009**, *1*, 65–90.
5. Guidi, L.; Stemmann, L.; Jackson, G.A.; Ibanez, F.; Claustre, H.; Legendre, L.; Picheral, M.; Gorsky, G. Effects of phytoplankton community on production, size and export of large aggregates: A world-ocean analysis. *Limnol. Oceanogr.* **2009**, *54*, 1951–1963.
6. Grossart, H.P.; Czub, G.; Simon, M. Algae–bacteria interactions and their effects on aggregation and organic matter flux in the sea. *Environ. Microbiol.* **2006**, *8*, 1074–1084.
7. Simon, H.; Lipsewers, Y.A.; Giebel, H.A.; Wiltshire, K.H.; Simon, M. Temperature effects on aggregation during a spring diatom bloom. *Limnol. Oceanogr.* **2014**, *59*, 2089–2100.
8. Beauvais, S.; Pedrotti, M.L.; Egge, J.; Iversen, K.; Marasé, C. Effects of turbulence on TEP dynamics under contrasting nutrient conditions: Implications for aggregation and sedimentation processes. *Mar. Ecol. Prog. Ser.* **2006**, *323*, 47–57.
9. Burns, W.G.; Marchetti, A.; Ziervogel, K. Enhanced formation of transparent exopolymer particles (TEP) under turbulence during phytoplankton growth. *J. Plankton Res.* **2019**, *41*, 349–361.
10. Kahl, L.A.; Vardi, A.; Schofield, O. Effects of phytoplankton physiology on export flux. *Mar. Ecol. Prog. Ser.* **2008**, *354*, 3–19.
11. Alldredge, A.L.; Passow, U.; Logan, B.E. The abundance and significance of a class of large, transparent organic particles in the ocean. *Deep Sea Res. Part I Oceanogr. Res. Pap.* **1993**, *40*, 1131–1140.
12. Mari, X.; Passow, U.; Migon, C.; Burd, A.B.; Legendre, L. Transparent exopolymer particles: Effects on carbon cycling in the ocean. *Prog. Oceanogr.* **2017**, *151*, 13–37.
13. Buesseler, K.O. The decoupling of production and particulate export in the surface ocean. *Glob. Biogeochem. Cycles* **1998**, *12*, 297–310.
14. Alldredge, A.L.; Gotschalk, C.; Passow, U.; Riebesell, U. Aggregation of diatom blooms: Insights from a mesocosm study. *Deep Sea Res. Part II Top. Stud. Oceanogr.* **1995**, *42*, 9–27.
15. Roca-Martí, M.; Puigcorbé, V.; Iversen, M.H.; Rutgers van der Loeff, M.; Klaas, C.; Cheah, W.; Bracher, A.; Masqué, P. High particulate organic carbon export during the decline of a vast diatom bloom in the Atlantic sector of the Southern Ocean. *Deep-Sea Res. II.* **2017**, *138*, 102–115.
16. Passow, U. Production of transparent exopolymer particles (TEP) by phyto- and bacterioplankton. *Mar. Ecol. Prog. Ser.* **2002**, *236*, 1–12.
17. Deng, W.; Cruz, B.N.; Neuer, S. Effects of nutrient limitation on cell growth, TEP production and aggregate formation of marine *Synechococcus*. *Aquat. Microb. Ecol.* **2016**, *78*, 39–49.
18. Chen, J.; Thornton, D.C.O. Transparent exopolymer particle production and aggregation by a marine planktonic diatom (*Thalassiosira weissflogii*) at different growth rates. *J. Phycol.* **2015**, *51*, 381–393.
19. Kiørboe, T.; Andersen, K.P.; Dam, H.G. Coagulation efficiency and aggregate formation in marine phytoplankton. *Mar. Biol.* **1990**, *107*, 235–245.

20. Engel, A.; Schartau, M. Influence of transparent exopolymer particles (TEP) on sinking velocity of *Nitzschia closterium* aggregates. *Mar. Ecol. Prog. Ser.* **1999**, *182*, 69–76.
21. Prairie, J.C.; Ziervogel, K.; Arnosti, C.; Camassa, R.; Falcon, C.; Khatri, S.; McLaughlin, R.M.; White, B.L.; Yu, S. Delayed settling of marine snow at sharp density transitions driven by fluid entrainment and diffusion-limited retention. *Mar. Ecol. Prog. Ser.* **2013**, *487*, 185–200.
22. Prairie, J.C.; Ziervogel, K.; Camassa, R.; McLaughlin, R.M.; White, B.L.; Dewald, C.; Arnosti, C. Delayed settling of marine snow: Effects of density gradient and particle properties and implications for carbon cycling. *Mar. Chem.* **2015**, *175*, 28–38.
23. Prairie, J.C.; White, B.L. A model for thin layer formation by delayed particle settling at sharp density gradients. *Cont. Shelf Res.* **2017**, *133*, 37–46.
24. MacIntyre, S.; Alldredge, A.L.; Gotschalk, C.C. Accumulation of marine snow at density discontinuities in the water column. *Limnol. Oceanogr.* **1995**, *40*, 449–468.
25. Shanks, A.L.; Edmondson, E.W. Laboratory-made artificial marine snow: A biological model of the real thing. *Mar. Biol.* **1989**, *101*, 463–470.
26. Ploug, H.; Iversen, M.H.; Fischer, G. Ballast, sinking velocity, and apparent diffusivity within marine snow and zooplankton fecal pellets: Implications for substrate turnover by attached bacteria. *Limnol. Oceanogr.* **2008**, *53*, 1878–1886.
27. Alldredge, A.L.; Gotschalk, C. In situ settling behavior of marine snow. *Limnol. Oceanogr.* **1988**, *33*, 339–351.
28. Passow, U.; Alldredge, A.L. A dye-binding assay for the spectrophotometric measurement of transparent exopolymer particles (TEP). *Limnol. Oceanogr.* **1995**, *40*, 1326–1335.
29. Passow, U. Transparent exopolymer particles (TEP) in aquatic environments. *Prog. Oceanogr.* **2002**, *55*, 287–333.
30. Azetsu-Scott, K.; Passow, U. Ascending marine particles: Significance of transparent exopolymer particles (TEP) in the upper ocean. *Limnol. Oceanogr.* **2004**, *49*, 741–748.
31. Seebah, S.; Fairfield, C.; Ullrich, M.S.; Passow, U. Aggregation and sedimentation of *Thalassiosira weissflogii* (diatom) in a warmer and more acidified future ocean. *PLoS ONE* **2014**, *9*, e112379.
32. Grossart, H.P.; Kiørboe, T.; Tang, K.W.; Allgaier, M.; Yam, E.M.; Ploug, H. Interactions between marine snow and heterotrophic bacteria: Aggregate formation and microbial dynamics. *Aquat. Microb. Ecol.* **2006**, *42*, 19–26.
33. Gärdes, A.; Iversen, M.H.; Grossart, H.P.; Passow, U.; Ullrich, M.S. Diatom-associated bacteria are required for aggregation of *Thalassiosira weissflogii*. *ISME J.* **2011**, *5*, 436–445.
34. Thornton, D. Diatom aggregation in the sea: Mechanisms and ecological implications. *Eur. J. Phycol.* **2002**, *37*, 149–161.
35. McDonnell, A.M.P.; Buesseler, K.O. Variability in the average sinking velocity of marine particles. *Limnol. Oceanogr.* **2010**, *55*, 2085–2096.
36. Villa-Alfageme, M.; de Soto, F.; Le Moigne, F.A.C.; Giering, S.L.C.; Sanders, R.; García-Tenorio, R. Observations and modeling of slow-sinking particles in the twilight zone. *Glob. Biogeochem. Cycles* **2014**, *28*, 1327–1342.
37. Passow, U. Formation of rapidly-sinking, oil-associated marine snow. *Deep Sea Res. Part II Top. Stud. Oceanogr.* **2016**, *129*, 232–240.
38. Porter, A.; Lyons, B.P.; Galloway, T.S.; Lewis, C. Role of marine snows in microplastic fate and bioavailability. *Environ. Sci. Technol.* **2018**, *52*, 7111–7119.
39. Katija, K.; Choy, C.A.; Sherlock, R.E.; Sherman, A.D.; Robison, B.H. From the surface to the seafloor: How giant larvaceans transport microplastics into the deep sea. *Sci. Adv.* **2017**, *3*, e1700715.
40. Prairie, J.C.; Ziervogel, K.; Camassa, R.; McLaughlin, R.M.; White, B.L.; Dewald, C.; Arnosti, C. Ephemeral aggregate layers in the water column leave lasting footprints in the carbon cycle. *Limnol. Oceanogr. Lett.* **2017**, *2*, 202–209.
41. Möller, K.O.; St. John, M.; Temming, A.; Floeter, J.; Sell, A.F.; Herrmann, J.P.; Möllmann, C. Marine snow, zooplankton and thin layers: Indications of a trophic link from small-scale sampling with the Video Plankton Recorder. *Mar. Ecol. Prog. Ser.* **2012**, *468*, 57–69.
42. Kiørboe, T.; Lundsgaard, C.; Olesen, M.; Hansen, J.L.S. Aggregation and sedimentation processes during a spring phytoplankton bloom: A field experiment to test coagulation theory. *J. Mar. Res.* **1994**, *52*, 297–323.

43. Thornton, D.C.O.; Thake, B. Effect of temperature on the aggregation of *Skeletonema costatum* (Bacillariophyceae) and the implication for carbon flux in coastal waters. *Mar. Ecol. Prog. Ser.* **1998**, *174*, 223–231.
44. Mari, X. Does ocean acidification induce an upward flux of marine aggregates? *Biogeosciences* **2008**, *5*, 1023–1031.
45. Cisternas-Novoa, C.; Lee, C.; Tang, T.; de Jesus, R.; Engel, A. Effects of higher CO_2 and temperature on exopolymer particle content and physical properties of marine aggregates. *Front. Mar. Sci.* **2019**, *5*, 500.